

Line-of-Sight Anisotropy of the 21cm Fluctuations Prior to Reionization

Rennan Barkana[†] & Abraham Loeb^{*}

[†] School of Physics and Astronomy, Sackler Faculty of Exact Sciences, Tel Aviv University, Tel Aviv 69978, ISRAEL

^{*} Astronomy Department, Harvard University, 60 Garden Street, Cambridge, MA 02138, USA

(February 7, 2020)

Between redshifts ~ 200 and ~ 25 , the adiabatically-cooling cosmic hydrogen absorbed the warmer microwave background at its resonant 21cm spin-flip transition. Subsequently, the gas was heated by radiation from the first galaxies and began to emit excess flux at this wavelength. Fluctuations in the 21cm flux were sourced by density inhomogeneities and by fluctuations in the radiation from galaxies until the completion of reionization at redshift ~ 6 . If the 21cm fluctuation power spectrum were isotropic, then the contributions of the various fluctuation mechanisms would combine and the interpretation of the total would be model dependent and subject to degeneracies. We show that peculiar velocities increase the power spectrum by a factor of ~ 2 compared to density fluctuations alone, and introduce an angular dependence in Fourier space. The resulting angular structure relative to the line of sight facilitates a simple separation of the power spectrum into several components, permitting an unambiguous determination of the primordial power spectrum of density fluctuations, and of the detailed properties of all other sources of 21cm fluctuations.

PACS numbers: 98.80.-k, 98.65.-r, 98.70.Vc, 95.30.Jx

Introduction. Following the recombination of protons and electrons less than a million years after the big bang, the universe was filled with neutral hydrogen (H I). Hundreds of millions of years later, the first galaxies started to reionize the cosmic gas [1]. The spectra of the farthest quasars indicate that reionization completed at a redshift $z \sim 6$, a billion years after the big bang [2–4]. So far, the history of the universe between the recombination epoch and the end of reionization has not been directly observed. The hyperfine spin-flip transition of H I at a wavelength of 21 cm provides the most promising tracer of the cosmic gas before the end of reionization. Several groups are currently engaged in the construction of low-frequency radio experiments that will be capable of detecting the diffuse 21cm radiation from $z \gtrsim 6$ [5]. Since this radiation interacts with H I through a resonant transition, any observed wavelength selects a redshift slice of the universe. Future measurements of the redshifted 21cm brightness as a function of observed wavelength and sky coordinates should provide a three-dimensional map of the cosmic H I [6,7]. Fluctuations in the 21cm brightness are sourced by primordial density inhomogeneities on all scales down to the cosmological Jeans mass, making 21cm the richest data set on the sky, exceeding by orders of magnitude all other cosmological probes [8].

The 21cm signal can be seen only from epochs during which the gas was largely neutral and deviated from thermal equilibrium relative to the cosmic microwave background (CMB). The signal vanished at redshifts $z \gtrsim 200$, when the small residual fraction of free electrons after cosmological recombination kept the gas kinetic temperature, T_k , close to the CMB temperature, T_γ . But between $200 \gtrsim z \gtrsim 30$ the gas cooled adiabatically, faster than the CMB, and atomic collisions kept the spin temperature of the hyperfine level population below T_γ , so that the gas appeared in absorption [9,8]. As the Hubble

expansion continued to rarefy the gas, radiative coupling of T_s to T_γ began to dominate over collisional coupling of T_s to T_k and the 21cm signal started to fade. As soon as the first galaxies formed, the UV photons they produced between the Ly α and Lyman limit wavelengths propagated freely through the universe, redshifted into the Ly α resonance, and coupled T_s and T_k once again through the Wouthuysen-Field [10,11] effect (by which the two hyperfine states are mixed through the absorption and re-emission of a Ly α photon). Emission of UV photons above the Lyman limit by the same galaxies initiated the process of reionization by creating ionized bubbles in the neutral gas around these galaxies. While UV photons were blocked by the neutral boundary of the bubbles, X-ray photons propagated farther into the bulk of the intergalactic gas and heated T_k above T_γ throughout the universe. Once T_s grew larger than T_γ , the gas appeared in 21cm emission. The ionized bubbles imprinted a knee in the power spectrum of 21cm fluctuations [12], which traced the H I topology as the ionized bubbles percolated and completed the process of reionization [13].

Spin temperature history. The spin temperature T_s is defined through the ratio between the number densities of hydrogen atoms in the excited and ground state levels, $n_1/n_0 = (g_1/g_0) \exp\{-T_\star/T_s\}$, where subscripts 1 and 0 correspond to the excited and ground state levels of the 21cm transition, $(g_1/g_0) = 3$ is the ratio of the spin degeneracy factors of the levels, and $T_\star = 0.0682\text{K}$ is the temperature corresponding to the energy difference between the levels. As long as T_s is smaller than the CMB temperature $T_\gamma = 2.725(1+z)$ K, hydrogen atoms absorb the CMB, whereas if $T_s > T_\gamma$ they emit excess flux above that of the CMB. In general, the resonant 21cm interaction changes the brightness temperature of the CMB by $T_b = \tau (T_s - T_\gamma) / (1+z)$. The optical depth for resonant absorption at a wavelength $\lambda = 21\text{cm}$ is

$$\tau = \frac{3c\lambda^2 h A_{10} n_H}{32\pi k_B T_s (1+z) (dv_r/dr)} x_{\text{HI}} , \quad (1)$$

where n_H is the number density of hydrogen, $A_{10} = 2.85 \times 10^{-15} \text{ s}^{-1}$ is the spontaneous emission coefficient, x_{HI} is the neutral hydrogen fraction, and dv_r/dr is the gradient of the radial velocity along the line of sight with v_r being the physical radial velocity and r the comoving distance; on average $dv_r/dr = H(z)/(1+z)$ where H is the Hubble parameter. The velocity gradient term arises since the 21cm scattering cross-section has a fixed thermal width which translates through the redshift factor $(1+v_r/c)$ to a fixed interval in velocity [14].

For the concordance set of cosmological parameters [15], the mean brightness temperature on the sky at redshift z is $T_b = 28 \text{ mK} [(1+z)/10]^{1/2} [(T_s - T_\gamma)/T_s] \bar{x}_{\text{HI}}$, where \bar{x}_{HI} is the mean neutral fraction of hydrogen. The spin temperature itself is coupled to T_k through the spin-flip transition, which can be excited by collisions or by the absorption of Ly α photons. As a result, the combination that appears in T_b becomes $(T_s - T_\gamma)/T_s = [x_{\text{tot}}/(1+x_{\text{tot}})] (1 - T_\gamma/T_k)$, where $x_{\text{tot}} = x_\alpha + x_c$ is the sum of the radiative and collisional threshold parameters. These parameters are $x_\alpha = 4P_\alpha T_\star/27A_{10}T_\gamma$ and $x_c = 4\kappa_{1-0}(T_k) n_H T_\star/3A_{10}T_\gamma$, where P_α is the Ly α scattering rate which is proportional to the Ly α intensity, and κ_{1-0} is tabulated as a function of T_k [16].

Brightness temperature fluctuations. Although the mean 21cm emission or absorption is difficult to measure due to bright foregrounds, the unique character of the fluctuations in T_b allows for a much easier extraction of the signal [12,17]. In general, the fluctuations in T_b can be sourced by fluctuations in gas density, temperature, neutral fraction, radial velocity gradient, and Ly α flux (through x_α). Adopting the notation δ_A for the fractional fluctuation in quantity A (with a lone δ denoting density perturbations), we find

$$\delta_{T_b} = \left(1 + \frac{x_c}{\tilde{x}_{\text{tot}}}\right) \delta + \frac{x_\alpha}{\tilde{x}_{\text{tot}}} \delta_{x_\alpha} + \delta_{x_{\text{HI}}} - \delta_{d_r v_r} + (\gamma_a - 1) \left[\frac{T_\gamma}{T_k - T_\gamma} + \frac{x_c}{\tilde{x}_{\text{tot}}} \frac{d \log(\kappa_{1-0})}{d \log(T_k)} \right] \delta , \quad (2)$$

where the adiabatic index is $\gamma_a = 1 + (\delta_{T_k}/\delta)$, and we define $\tilde{x}_{\text{tot}} \equiv (1+x_{\text{tot}})x_{\text{tot}}$. Taking the Fourier transform, we obtain the power spectrum of each quantity; e.g., the total power spectrum P_{T_b} is defined by

$$\langle \tilde{\delta}_{T_b}(\mathbf{k}_1) \tilde{\delta}_{T_b}(\mathbf{k}_2) \rangle = (2\pi)^3 \delta^D(\mathbf{k}_1 + \mathbf{k}_2) P_{T_b}(\mathbf{k}_1) , \quad (3)$$

where $\tilde{\delta}_{T_b}(\mathbf{k})$ is the Fourier transform of δ_{T_b} , \mathbf{k} is the comoving wavevector, and $\langle \dots \rangle$ denotes an ensemble average.

The separation of powers. The fluctuation δ_{T_b} consists of a number of isotropic sources of fluctuations plus the peculiar velocity term $-\delta_{d_r v_r}$. Since this term involves radial projections, it inserts an anisotropy into the

power spectrum. Its Fourier transform is simply proportional to that of the density field [18],

$$\tilde{\delta}_{d_r v_r} = -\mu^2 \tilde{\delta} , \quad (4)$$

where $\mu = \cos \theta_k$ in terms of the angle θ_k of \mathbf{k} with respect to the line of sight. The μ^2 dependence in this equation results from taking the radial component ($\propto \mu$) of the peculiar velocity, and then the radial component ($\propto \mu$) of its gradient. Intuitively, a high-density region possesses a velocity infall towards the density peak, implying that a photon must travel further from the peak in order to reach a fixed relative redshift, compared with the case of pure Hubble expansion. Thus the optical depth is always increased by this effect in regions with $\delta > 0$. This phenomenon is most properly termed *velocity compression*.

We therefore write the fluctuation in Fourier space as

$$\tilde{\delta}_{T_b}(\mathbf{k}) = \mu^2 \tilde{\delta}(\mathbf{k}) + \beta \tilde{\delta}(\mathbf{k}) + \tilde{\delta}_{\text{rad}}(\mathbf{k}) , \quad (5)$$

where we have defined a coefficient β by collecting all terms $\propto \delta$ in Eq. (2), and have also combined the terms that depend on the radiation fields of Ly α photons and ionizing photons, respectively. We assume that these radiation fields produce isotropic power spectra, since the physical processes that determine them have no preferred direction in space. The total power spectrum is

$$P_{T_b}(\mathbf{k}) = \mu^4 P_\delta(k) + 2\mu^2 [\beta P_\delta(k) + P_{\delta-\text{rad}}(k)] + [\beta^2 P_\delta(k) + P_{\text{rad}}(k) + 2\beta P_{\delta-\text{rad}}(k)] , \quad (6)$$

where we have defined the power spectrum $P_{\delta-\text{rad}}$ as the Fourier transform of the cross-correlation function,

$$\xi_{\delta-\text{rad}}(r) = \langle \delta(\mathbf{r}_1) \delta_{\text{rad}}(\mathbf{r}_1 + \mathbf{r}) \rangle . \quad (7)$$

We may now calculate the angular power spectrum of the brightness temperature on the sky at a given redshift – corresponding to a comoving distance r_0 along the line of sight. The brightness fluctuations can be expanded in spherical harmonics with expansion coefficients $a_{lm}(\nu)$, where the angular power spectrum

$$C_l(r_0) = \langle |a_{lm}(\nu)|^2 \rangle = 4\pi \int \frac{d^3 k}{(2\pi)^3} \left[G_l^2(kr_0) P_\delta(k) + 2P_{\delta-\text{rad}}(k) G_l(kr_0) j_l(kr_0) + P_{\text{rad}}(k) j_l^2(kr_0) \right] , \quad (8)$$

with $G_l(x) \equiv J_l(x) + (\beta - 1) j_l(x)$ and $J_l(x)$ being a linear combination of spherical Bessel functions [18].

The velocity gradient term has been previously neglected in calculations of the 21cm fluctuations, except for its effect on the sky-averaged power and on radio visibilities [18]. In the simple case where only the velocity term contributes along with density fluctuations and $\beta = 1$, the velocity term increases the total power by a factor of $\langle (1 + \mu^2)^2 \rangle = 1.87$ in the spherical average. However, instead of averaging the signal, we

can use the angular structure of the power spectrum to greatly increase the discriminatory power of 21cm observations. Rather than averaging the observations over spherical shells in \mathbf{k} space, we may instead break up each shell into rings of constant μ and construct the observed $P_{T_b}(k, \mu)$. Considering Eq. (6) as a polynomial in μ , i.e., $\mu^4 P_{\mu^4} + \mu^2 P_{\mu^2} + P_{\mu^0}$, we see that the power at just three values of μ is required in order to separate out the coefficients of 1, μ^2 , and μ^4 for each k .

If the velocity compression were not present, then only the μ -independent term (times T_b^2) would be observed, and its separation into the five components (T_b , β , and three power spectra) would be difficult and subject to degeneracies. Once the power has been separated into three parts, however, the μ^4 coefficient can be used to measure the density power spectrum directly, with no interference from any other source of fluctuations. Since the overall amplitude of the power spectrum, and its scaling with redshift, are well determined from the combination of the CMB temperature fluctuations and galaxy surveys, the amplitude of P_{μ^4} directly determines the mean brightness temperature T_b on the sky, which measures a combination of T_s and \bar{x}_{HI} at the observed redshift. Once $P_\delta(k)$ has been determined, the coefficients of the μ^2 term and the μ -independent term must be used to determine the remaining unknowns, β , $P_{\delta-\text{rad}}(k)$, and $P_{\text{rad}}(k)$. Since the coefficient β is independent of k , determining it and thus breaking the last remaining degeneracy requires only a weak additional assumption on the behavior of the power spectra, such as their asymptotic behavior at large or small scales. If the measurements cover N_k values of wavenumber k , then one wishes to determine $2N_k + 1$ quantities based on $2N_k$ measurements, which should not cause significant degeneracies when $N_k \gg 1$. Even without knowing β , one can probe whether some sources of $P_{\text{rad}}(k)$ are uncorrelated with δ ; the quantity $P_{\text{un}-\delta}(k) \equiv P_{\mu^0} - P_{\mu^2}^2 / (4P_{\mu^4})$ equals $P_{\text{rad}} - P_{\delta-\text{rad}}^2 / P_\delta$, which receives no contribution from any source that is a linear functional of the density distribution.

Specific epochs. At $z \sim 35$, galaxy formation is in its infancy, while collisions are effective due to the high gas density [8]. Thus, $x_{\text{tot}} = x_c \gg x_\alpha$, $x_{\text{HI}} = 1$, and the gas cools adiabatically (with $\gamma_a = 5/3$). In addition to measuring the density power spectrum [8], one can also measure T_s and β , which depend only on the mean values of n_{HI} , T_γ , T_k and on known atomic physics. It is possible to trace the redshift evolution of these quantities and verify that collisions are causing the fluctuations, using the independent measurement of β^2 from $P_{\mu^0}(k)$.

At $z \lesssim 35$, collisions become ineffective but the first stars produce a cosmic background of Ly α photons that couples T_s to T_k . During the period of initial Ly α coupling, fluctuations in the Ly α flux translate into fluctuations in the 21cm brightness [19]. This signal can be observed from $z \sim 25$ until the Ly α coupling is completed (i.e., $x_{\text{tot}} \gg 1$) at $z \sim 15$. At a given redshift, each atom

sees Ly α photons that were originally emitted at earlier times at rest-frame wavelengths between Ly α and the Lyman limit. Distant sources are time retarded, and since there are fewer galaxies in the distant, earlier universe, each atom sees sources only out to an apparent source horizon of ~ 100 comoving Mpc at $z \sim 20$. A significant portion of the flux comes from nearby sources, because of the $1/r^2$ decline of flux with distance, and since higher Lyman series photons, which are degraded to Ly α photons through scattering, can only be seen from a small redshift interval that corresponds to the wavelength interval between two consecutive atomic levels.

There are two separate sources of fluctuations in the Ly α flux [19]. The first is density inhomogeneities. Since gravitational instability proceeds faster in overdense regions, the biased distribution of rare galactic halos fluctuates much more than the global dark matter density. When the number of sources seen by each atom is relatively small, Poisson fluctuations provide a second source of fluctuations, statistically independent to first order. Unlike typical Poisson noise, these fluctuations are correlated between gas elements at different places, since two nearby elements see many of the same sources, at about the same distance. Assuming a scale-invariant spectrum of primordial density fluctuations, and that $x_\alpha = 1$ is produced at $z = 20$ by galaxies in dark matter halos where the gas cools efficiently via atomic cooling, we show in Figure 1 the predicted observable power spectra. The figure shows that β can be measured from the ratio P_{μ^2}/P_{μ^4} at $k \gtrsim 1 \text{ Mpc}^{-1}$, allowing the density-induced fluctuations in flux to be extracted from P_{μ^2} , while only the Poisson fluctuations contribute to $P_{\text{un}-\delta}$. Each of these components probes the number density of galaxies through its magnitude, and the distribution of source distances through its shape. Measurements at $k \gtrsim 100 \text{ Mpc}^{-1}$ can independently probe T_k because of the smoothing effects of the gas pressure and the thermal width of the 21cm line.

After Ly α coupling and X-ray heating are both completed, reionization of the intergalactic hydrogen continues and $\delta_{x_{\text{HI}}}$ increases. Since $\beta = 1$ and $T_k \gg T_\gamma$, the normalization of P_{μ^4} directly measures the mean neutral hydrogen fraction, and one can separately probe the density fluctuations, the neutral hydrogen fluctuations, and their cross-correlation.

Fluctuations on large angular scales. Full-sky observations must normally be analyzed with an angular and radial transform, rather than a Fourier transform which is simpler and yields more directly the underlying 3D power spectrum. In an angular transform on the sky, an angle of θ radians translates to a spherical multipole $l \sim 3.5/\theta$. For measurements on a screen at a comoving distance of $r_0(z)$, a multipole l normally measures 3D power on a scale of $k^{-1} \sim \theta r_0 \sim 35/l \text{ Gpc}$ for $l \gg 1$, since $r_0 \sim 10 \text{ Gpc}$ at $z \gtrsim 10$. This estimate fails at $l \lesssim 100$, however, when we consider the sources of 21cm fluctu-

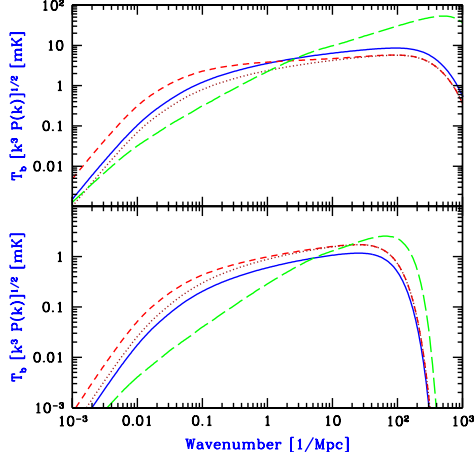


FIG. 1. Observable power spectra during the period of initial Ly α coupling. *Upper panel*: Assumes adiabatic cooling. *Lower panel*: Assumes pre-heating to 500 K by X-ray sources. We show $P_{\mu^4} = P_\delta$ (solid curves), P_{μ^2} (short-dashed curves), and $P_{\text{un}-\delta}$ (long-dashed curves). We also show for comparison $2\beta P_\delta$ (dotted curves).

ations. The angular projection implied in C_l involves a weighted average [Eq. (8)] which favors large scales when l is small, but density fluctuations possess little large-scale power, and the C_l are dominated by power around the peak of $kP_\delta(k)$, at a few tens of comoving Mpc.

Figure 2 shows that for density and velocity fluctuations, even the $l = 1$ multipole is affected by power at $k^{-1} > 200$ Mpc only at the 2% level. Due to the small number of large angular modes available on the sky, the expectation value of C_l cannot be measured precisely at small l . Figure 2 shows that this precludes new information from being obtained on scales $k^{-1} \gtrsim 130$ Mpc using angular structure at any given redshift. An optimal observing strategy would be to divide the sky into separate angular pixels of size $\theta \lesssim 2^\circ$, in which the curvature changes distances by only $\theta^2/24 \sim 7 \times 10^{-5}$. This would allow a direct 3D Fourier transform, which is also the most natural way of analyzing radio observations [17].

Acknowledgments. This work was supported in part by NSF grants AST-0204514, AST-0071019 and NASA grant NAG 5-13292. R.B. is grateful for the kind hospitality of the Harvard-Smithsonian CfA, and acknowledges the support of an Alon Fellowship at Tel Aviv University and of Israel Science Foundation grant 28/02/01.

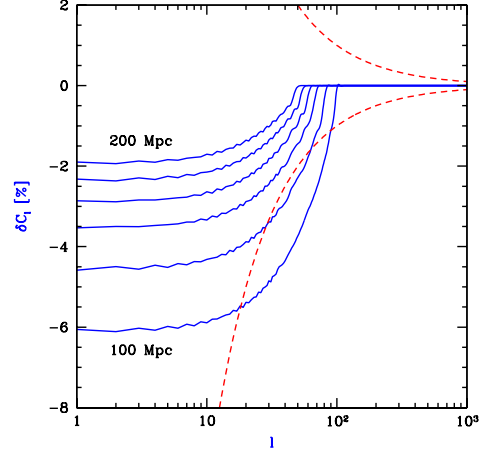


FIG. 2. Effect of large-scale power on the angular power spectrum of 21cm anisotropies on the sky. This example shows the power from density fluctuations and velocity compression, assuming a hot IGM at $z = 12$ with $T_s = T_k \gg T_\gamma$. We show the % change in C_l if we were to cut off the power spectrum above $1/k$ of 200, 180, 160, 140, 120, and 100 Mpc (top to bottom). Also shown for comparison is the cosmic variance for averaging in bands of $\Delta l \sim l$ (dashed lines).

- [3] R. L. White, R.H. Becker, X. Fan, & M.A. Strauss, *Astron. J.* **126**, 1 (2003).
- [4] J.S.B. Wyithe, & A. Loeb, *Nature* **427**, 815, (2004).
- [5] See Proc. of the *Epoch Of Reionization* Workshop at <http://space.mit.edu/eor-workshop/> (2004).
- [6] C. J. Hogan, & M.J. Rees, *Mon. Not. R. Astr. Soc.* **188**, 791 (1979).
- [7] P. Madau, A. Meiksin, & M. J. Rees, *Astrophys. J.* **475**, 429 (1997).
- [8] A. Loeb, & M. Zaldarriaga, *Phys. Rev. Lett.* **92**, 211301 (2004).
- [9] D. Scott, & M. J. Rees, *Mon. Not. R. Astr. Soc.* **247**, 510 (1990).
- [10] S. A. Wouthuysen, *Astron. J.* **57**, 31 (1952).
- [11] G. B. Field, *Proc. IRE* **46**, 240 (1958).
- [12] M. Zaldarriaga, S. R. Furlanetto, & L. Hernquist, *Astrophys. J.* **608**, 622 (2004).
- [13] S. Furlanetto, M. Zaldarriaga, & L. Hernquist, *Astrophys. J.*, submitted, preprint [astro-ph/0403697] (2004).
- [14] V. V. Sobolev, *Moving Envelopes of Stars*, Cambridge: Harvard University Press (1960)
- [15] D. N. Spergel, et al., *Astrophys. J. Suppl.* **148**, 175 (2003).
- [16] A. C. Allison, & A. Dalgarno, *Astrophys. J.* **158**, 423 (1969); B. Zygelman, & A. Dalgarno, in preparation.
- [17] M. F. Morales, & J. Hewitt, *Astrophys. J.*, in press, preprint [astro-ph/0312437] (2004); M. F. Morales, *Astrophys. J.*, submitted, preprint [astro-ph/0406662] (2004).
- [18] S. Bharadwaj, & S. S. Ali, *Mon. Not. R. Astr. Soc.* **352**, 142 (2004); S. Bharadwaj, & S. S. Ali, *Mon. Not. R. Astr. Soc.*, submitted, preprint [astro-ph/0406676] (2004).
- [19] R. Barkana, & A. Loeb, *Astrophys. J. Lett.*, submitted.

[1] R. Barkana, & A. Loeb, *Phys. Rep.* **349**, 125 (2001).
[2] X. Fan, et al., *Astron. J.* **123**, 1247 (2002).